



# Synthesis and characterization of the *n*-butyl palmitate as an organic phase change material

Liyun Ma<sup>1</sup> · Chuigen Guo<sup>1</sup> · Rongxian Ou<sup>1</sup> · Qingwen Wang<sup>1</sup> · Liping Li<sup>1</sup>

Received: 3 July 2018 / Accepted: 16 October 2018  
© Akadémiai Kiadó, Budapest, Hungary 2018

## Abstract

In this research, the *n*-butyl palmitate was synthesized using the esterification reaction of the PA with *n*-butanol. The <sup>1</sup>H nuclear magnetic resonance and Fourier transform infrared illustrated that the hydroxyl group and carboxyl group disappeared, and the ester bond appeared after the reaction, explaining that *n*-butyl palmitate was successfully fabricated. The differential scanning calorimetry indicated that the phase-transition temperature and latent heat are 12.6 °C and 127.1 J g<sup>-1</sup>, which was suited to use in low-temperature fields such as food, pharmaceutical, and biomedical. The thermogravimetric analysis suggested that it had great thermal stability during the phase change process. In addition, the thermal conductivity of the *n*-butyl palmitate was slightly higher than other fatty acid ester, and the 500 thermal cycles test results indicated that it had excellent thermal reliability. Therefore, the *n*-butyl palmitate is deduced to share great thermal energy storage ability in terms of latent heat thermal energy system applications.

**Keywords** Palmitic acid ester · Phase change material · Esterification · Thermal energy storage

## Introduction

At present, the secondary energy such as the wasted heat from industry, solar power, surface heat, and others still exists many problems, which have low utilization efficiency, poor economic benefit and other major issues. Many scholars have found that phase change energy storage technology is an effective means to enhance energy utilization and economic benefit by using phase change materials (PCMs) [1], which is a kind of material that can absorb thermal energy from the environment and release the thermal energy to the environment during the phase change process, to achieve the purpose of thermal storage and release. Most of PCMs, such as organic PCMs [2], inorganic PCMs [3], or their eutectic mixtures [4] have been extensively studied as latent heat storage materials for decades. And it has been applied in the solar water-heating

systems [5], building [6], and air conditioning systems [7] due to high energy storage density and repeatable utilization property [8]. Among the previous reports [9–11], fatty acids PCMs have been widely investigated as a superior kind of phase change material (PCM).

However, fatty acid ester PCM was relatively much less studied. From the previous study [12–15], the fatty acid ester can be fabricated by direct esterification reaction of fatty acids with alcohols. It has a high latent heat and a suitable phase-transition temperature as a PCM. Feldman et al. [12] considered esters to be promising storage media candidates for latent heat storage systems as they show little to no supercooling, high chemical and thermal stability, and no corrosiveness. Afterwards, Karaipekli et al. [13] discovered that several fatty acid esters equipped with great phase change properties, and the phase-transition temperatures and the latent heats of them were in the range of 21.6–32.3 °C and 35.9–43.3 J g<sup>-1</sup>, respectively. Sari et al. [14] reported that the stearic acid, myristic acid, and palmitic acid were combined with glycerol to synthesize fatty acid esters through the reaction of Fischer esterification. They were characterized by the <sup>1</sup>H nuclear magnetic resonance (<sup>1</sup>H NMR), Fourier transform infrared (FT-IR), and differential scanning calorimetry

✉ Qingwen Wang  
qwwang@scau.edu.cn

✉ Liping Li  
lilipinguo@126.com

<sup>1</sup> College of Materials and Energy, South China Agricultural University, Guangzhou 510642, People's Republic of China

(DSC). The test outcome suggested that the latent heats of synthesized esters were around 149–185 J g<sup>-1</sup>, and the phase-transition temperatures were found in the range of 31–63.1 °C, illustrating that they had optimum properties. Sari et al. [15] also investigated that the erythritol with the melting temperature of 118.4 °C served as alcohol, the palmitic acid (PA) and stearic acid (SA) with the phase-transition temperatures of 62.74 °C and 68.86 °C acted as acids, the erythritol palmitate and erythritol stearate were prepared by the esterification reaction. The results showed that the phase-transition temperatures of these two esters were 21.93 °C and 30.35 °C, respectively. It also had good thermal reliability, chemical stability, and physical properties.

Among the fatty acid PCMs, the PA has very superior performance, such as suitable phase-transition temperature, high latent heat, and excellent chemical stability, etc. [16]. It has a strong application potential as a PCM such as water-heating systems and others high-temperature filed [5]. However, the PA is limited in some practical field such as solar heating-cooling of buildings and smart textile due to the high phase-transition temperature [17].

To overcome the above-mentioned issues, the PA ester was synthesized as a PCM. In this study, a kind of PA ester called *n*-butyl palmitate was obtained successfully by using the esterification reaction between the PA and *n*-butanol. The chemical structures of the PA, *n*-butanol, and the obtained *n*-butyl palmitate were analyzed by the FT-IR, and the esterification reaction was investigated by the <sup>1</sup>H NMR technique. The thermal property of the *n*-butyl palmitate was characterized by using the DSC and thermogravimetric analysis (TG). The Hot-disk thermal constants analyzer was employed to measure the thermal conductivity of *n*-butyl palmitate. After 500 thermal cycles, the DSC and FT-IR analyses were duplicated to find out the change of phase change property and chemical structure of the PA ester.

## Experimental

### Materials

PA (C<sub>16</sub>H<sub>32</sub>O<sub>2</sub>) was supplied by Kermel Chemical Reagent Co., Ltd., Tianjin, China. *n*-Butanol (C<sub>4</sub>H<sub>10</sub>O) was purchased from Guangzhou Chemical Reagent Factory, China. P-toluenesulfonic acid (TsOH, p-CH<sub>3</sub>C<sub>6</sub>H<sub>4</sub>SO<sub>3</sub>H) was bought from Guangzhou Jinhuda Chemical Reagent Co., Ltd., China, which acted as the catalyst. Benzene was provided from Tianjin Damao Chemical Reagent Co., Ltd., China, which served as water-carrying agent to separate the water that generated in the reaction. Anhydrous sodium sulphate as a desiccant was supplied by Guangzhou

Chemical Reagent Factory, China. All of the above chemical materials were analytical grade reagent.

### Fabrication of *n*-butyl palmitate

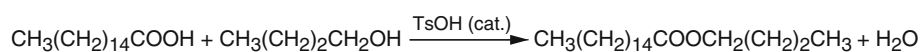
The *n*-butyl palmitate was done in accordance to the method of the esterification reaction, which was conducted by taking the calculated amount of PA and *n*-butanol (molar ratio: 1:1 for PA:*n*-butanol) in benzene and a flask with a reflux condenser and numerical show constant temperature oil-bathing (the Jiang Su Ke Xi Instrument Co., Ltd., China). Then, the catalyst p-toluenesulfonic acid was added when the PA was melted thoroughly. Following, the mixture was unremittingly stirred at the temperature of 120 °C for 1.5 h in the oil-bathing with a mechanical stirrer. Water in the reaction medium was gradually removed by benzene using the distillation method. Afterwards, the product was slowly cooled down to crystal completely. Finally, the as-prepared *n*-butyl palmitate was purified in acetone solution with agitation for 30 min and then distilled to remove acetone. Subsequently, it was dried using anhydrous sodium sulphate. In the end, the *n*-butyl palmitate was fabricated successfully. The reaction scheme is shown in Scheme. 1.

### Characterization

To verify the properties of the *n*-butyl palmitate, the prepared *n*-butyl palmitate and its components were systematically characterized. The physicochemical compatibility of the components for the *n*-butyl palmitate with each other was investigated by the FT-IR (Perkin Elmer Spectrum 100; USA) on a KBr pellet at the wavenumber range from 400 to 4000 cm<sup>-1</sup>. The chemical bond and proton number of the *n*-butyl palmitate were conducted by the <sup>1</sup>H NMR spectrum (Varian 400MR; USA). The <sup>1</sup>H NMR spectrum of the *n*-butyl palmitate was obtained at the frequency of 400 MHz, and it was dissolved in acetone-d<sub>6</sub> (C<sub>3</sub>D<sub>6</sub>O) with a concentration of 100 mg 0.5 mL<sup>-1</sup> [18].

The temperatures related with melting and crystallization and phase change latent heat values of melting and cooling were determined for the PA and its esters via the DSC (NETZSCH STA-449C model instrument, Germany) in the range of 253–373 K. For the measurement, the aluminum crucible was filled with the samples around 5 mg. All of the DSC measurements were conducted at a melting/cooling rate of 3 K min<sup>-1</sup>, under the static nitrogen atmosphere of 20 mL min<sup>-1</sup>. All the experiments and each sample were required to be measured twice, while the average values were put into use.

The thermal stability of *n*-butyl palmitate was carried out using a TG (NETZSCH TG 209 model instrument, Germany) under a static nitrogen atmosphere of



**Scheme 1** The esterification reaction of the PA with *n*-butanol

20 mL min<sup>-1</sup>, at a heating scanning rate of 10 K min<sup>-1</sup>. The mass of the samples was put into alumina crucible and kept within 8–12 mg for the measurement in the temperature range of 303–873 K [19]. The thermal conductivity of *n*-butyl palmitate was detected by using the Hot-disk thermal constants analyzer (Hot-disk Tp2500S; Sweden) at ambient temperature.

The thermal reliability is one of the essential parameters of PCMs. To make sure a good thermal reliability of the *n*-butyl palmitate, performing an accelerated test in terms of thermal cycling was necessary. It was as follows: the *n*-butyl palmitate was put into a thermostatic chamber. Then, it was heated above the melting temperature and cooled under the crystallization temperature. Thus a thermal cycle was completed including a melting and cooling process [20]. It is required that the procedure is scheduled to be continuously repeated 500 times. Finally, the variations of phase change property and chemical structure of thermal cycling treated sample were examined by the DSC and FT-IR, respectively [21].

## Results and discussion

### The chemical property of the synthesized *n*-butyl palmitate as a PCM

Among PCMs, the synthesized *n*-butyl palmitate was determined by using the <sup>1</sup>H NMR and FT-IR method. The FT-IR characteristic peaks of the PA, *n*-butanol, and *n*-butyl palmitate were shown in Fig. 1. At the FT-IR spectrum of the PA, the characteristic bands appeared at 3443, 2921, 2850, 1703, 1467, 1294, 941, and 720 cm<sup>-1</sup>. The peak at 3443 cm<sup>-1</sup> exhibited in the spectrum of PA indicates the stretching vibrations of the hydroxyl group. The peaks at 2921 cm<sup>-1</sup> and 2850 cm<sup>-1</sup> represent the stretching vibration of –CH<sub>3</sub> and –CH<sub>2</sub> group. The peak at 1703 cm<sup>-1</sup> represents the stretching vibration of C=O. What the absorption band at 1467 cm<sup>-1</sup> is attributed to –CH<sub>2</sub> asymmetrical bending vibration. The characteristic absorption bands at 941 cm<sup>-1</sup> and 720 cm<sup>-1</sup> are associated with the out-of-plane bending vibration and the in-plane swinging vibration of the hydroxyl group, respectively [16].

As for the *n*-butanol, the characteristic peaks are much less due to the short molecular chain. The peak at 3361 cm<sup>-1</sup> exhibited in the spectrum of the *n*-butanol indicates the stretching vibrations of the hydroxyl group.

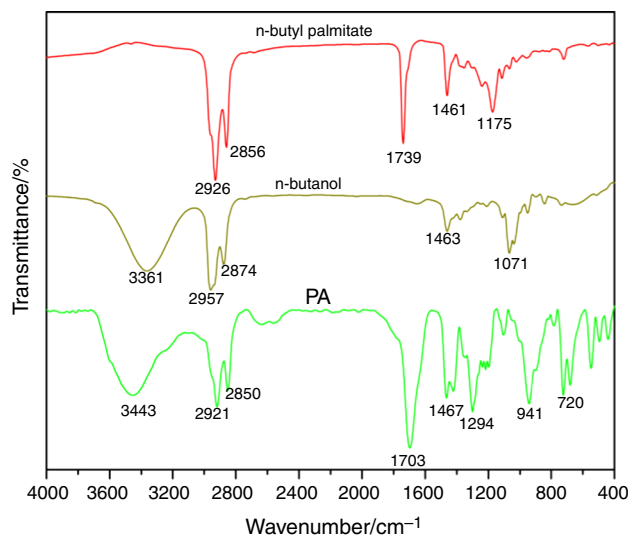


**Fig. 1** FTIR spectra of the PA, *n*-butanol, and *n*-butyl palmitate

The characteristic absorption bands at 2957 and 2874 cm<sup>-1</sup> correspond to the –CH<sub>3</sub> and –CH<sub>2</sub> stretching vibration. The characteristic peak exhibited at 1463 cm<sup>-1</sup> is CH<sub>2</sub> asymmetrical bending vibration. The absorption peak emerged at 1071 cm<sup>-1</sup> is assigned to stretching vibration of the C–O group.

However, as for the *n*-butyl palmitate, the carboxylic acid and hydroxy absorption peaks at 3443 and 3361 cm<sup>-1</sup> have disappeared, which indicated that the carboxylic acid groups of PA and hydroxyl of the *n*-butanol have transformed into ester bond. As a result, the characteristic peaks exhibited at 1739 cm<sup>-1</sup> signifies stretching vibration of the C=O groups of the *n*-butyl palmitate. The peak located at 1175 cm<sup>-1</sup> is assigned to stretching vibration of the C–O–C band for the *n*-butyl palmitate. In conclusion, the *n*-butyl palmitate was successfully synthesized.

The <sup>1</sup>H NMR spectrum of *n*-butyl palmitate was shown in Fig. 2. There was no peak of –OH group at about 2.24 ppm for the *n*-butanol. Furthermore, the proton of –COO–CH<sub>2</sub>– which is at 4.03 ppm for *n*-butyl palmitate is related to the appearance of the peak, which play a role in illustrating the esterification reaction, proved to be successful. The number of H proton and chemical shift were in accordance with the *n*-butyl palmitate, and all of the above results verify that the *n*-butyl palmitate was also synthesized.

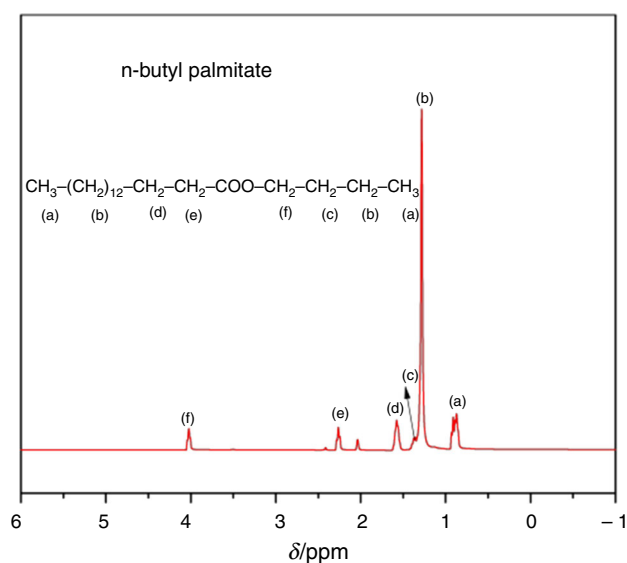


Fig. 2  $^1\text{H}$  NMR spectrum of the *n*-butyl palmitate

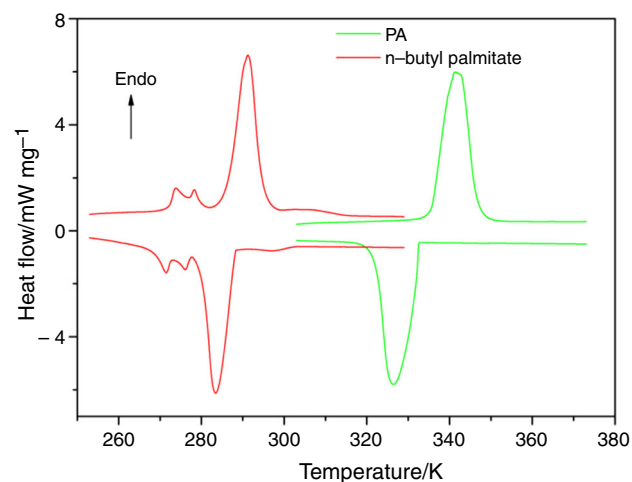


Fig. 3 DSC curves of the PA and *n*-butyl palmitate

### Thermal property of the synthesized *n*-butyl palmitate as a PCM

The DSC curves of the PA and *n*-butyl palmitate were illustrated in Fig. 3. The DSC results were listed in Table 1. The definition of phase change temperature and the latent heat ( $\Delta H$ ) were reported in our previous study [11]. From the Fig. 3 and Table 1, the melting temperature of the PA was higher than the *n*-butyl palmitate's. The latent heat value of *n*-butyl palmitate was lower than the PA's. However, these values obtained from DSC analysis were still high enough to be a PCM for the latent heat thermal energy system (LHTES) applications. Therefore, it can be concluded that the *n*-butyl palmitate is well suited as a PCM due to the high phase latent heat and a

Table 1 Thermal characteristics of the PA and *n*-butyl palmitate

|                           | Melting process |                              | Cooling process |                              |
|---------------------------|-----------------|------------------------------|-----------------|------------------------------|
|                           | $T_m/\text{K}$  | $\Delta H_m/\text{J g}^{-1}$ | $T_c/\text{K}$  | $\Delta H_c/\text{J g}^{-1}$ |
| PA                        | 335.6           | 212.8                        | 332.5           | 216.1                        |
| <i>n</i> -Butyl palmitate | 285.6           | 127.1                        | 285.7           | 134.5                        |

suitable melting temperature. As seen in Table 1, the melting temperature of PA that is 335.6 K could not be discovered in *n*-butyl palmitate; this confirmed that there was no residual PA in the prepared *n*-butyl palmitate. The melting and crystallization temperatures of the *n*-butyl palmitate are 285.6 K and 285.7 K, respectively. The phase change latent heats of melting and crystallization of the *n*-butyl palmitate are 127.1 J g $^{-1}$  and 134.5 J g $^{-1}$ , respectively. These properties make them become a promising PCM to storage and release thermal energy for the LHTES applications. In a word, these measurement results also suggested that the highest potential of *n*-butyl palmitate lies in low-temperature application such as food, pharmaceutical, and biomedical [1].

### Thermal conductivity of the synthesized *n*-butyl palmitate as a PCM

To become a PCM which was widely used in the LHTES applications, the thermal conductivity is an important parameter, because the thermal conductivity of the PCM directly affects the rate of thermal energy storage and release [22]. The thermal energy storage and release could not be achieved entirely if the thermal conductivity was very low. The previous studies [16] reported that the thermal conductivity of the PA was 0.17 W m $^{-1}$  K $^{-1}$ , which was too low to be directly used in many fields. So the high thermal conductivity materials (2–400 W m $^{-1}$  K $^{-1}$ ) were added to PCMs to enhance thermal conductivity. The previous works [21, 23, 24] reported that the activated carbon, expanded graphite, carbon fiber, and graphene were added to the PCM, exhibiting a superior thermal conductivity.

The thermal conductivity of the *n*-butyl palmitate was measured at the room temperature as 0.25 W m $^{-1}$  K $^{-1}$  (Fig. 4). Although it was higher than the PA, it was still too low to be used in practical applications. Some materials with high thermal conductivity (expand graphite, graphene, carbon nanotube, etc.) can be added to the *n*-butyl palmitate to enhance the thermal conductivity and expand utilization of the *n*-butyl palmitate. As a result, without affecting the thermal properties and physicochemical properties of the *n*-butyl palmitate, the thermal conductivity of the *n*-butyl palmitate should be increased as much

as possible. Moreover, it has been shown in Table 2 about the results of thermal conductivity in terms of *n*-butyl palmitate with that from some fatty acid ester in the literature [1, 14, 15, 25]. By comparing these data, it can be noted that the *n*-butyl palmitate in this study has the slightly higher thermal conductivity than those reported fatty acid ester due to the different test conditions and methods, crystallinity, and molecular chain orientation. As a result, the synthesized *n*-butyl palmitate as an organic PCM had great ability in terms of thermal energy storage for the LHTES applications.

### Thermal stability of the synthesized *n*-butyl palmitate as a PCM

The TG as well as derivative TG (DTG) curves which belongs to the PA and *n*-butyl palmitate has been shown in Fig. 5. The analysis method is referred to the previous report [26, 27]. As can be seen from the Fig. 5, the mass loss temperatures (at 5% degradation) of the PA and *n*-butyl palmitate occurred at 477.4 K and 436.6 K, respectively. The maximum degraded temperatures of the PA and *n*-butyl palmitate occurred at 540.6 K and 524.9 K, respectively. The appeared mass loss was attributed to the degradation of the PA and *n*-butyl palmitate. The mass losses of the PA and *n*-butyl palmitate are approximately

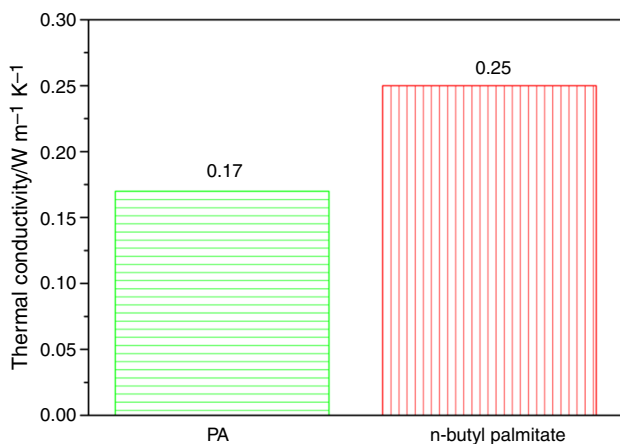


Fig. 4 Thermal conductivities of the PA and *n*-butyl palmitate

**Table 2** Comparison of thermal conductivity of *n*-butyl palmitate with that of fatty acid ester in the literatures

| Fatty acid esters         | Thermal conductivities/<br>$W m^{-1} K^{-1}$ |  | References |  |
|---------------------------|--|--|------------|--|
|                           |  |  |            |  |
| Glycerol tripalmitate     | 0.17   |  | [14]       |  |
| Erythritol tetrapalmitate | 0.16   |  | [15]       |  |
| Galactitol hexa palmitate | 0.19   |  | [1]        |  |
| Butyl stearate            | 0.23   |  | [25]       |  |
| <i>n</i> -Butyl palmitate | 0.25   |  | This work  |  |

100%. However, the *n*-butyl palmitate still had superior thermal stability during the phase change process due to its phase-transition temperature below the 436.6 K.

### Thermal reliability of synthesized *n*-butyl palmitate as a PCM

A PCM must be thermally and chemically stable over a large number of melting and freezing cycling. Therefore, it was absolutely essential for no or less change in its properties in the long-term using process [16]. Thermal cycling test was carried out to verify the change in thermal properties of the *n*-butyl palmitate with concerning 500 thermal cycles and the results were shown in Table 3. Figure 6 depicts the DSC curves of *n*-butyl palmitate before and after 500 thermal cycles. From the DSC curves, it is a little changed for the melting temperature and latent heat. The

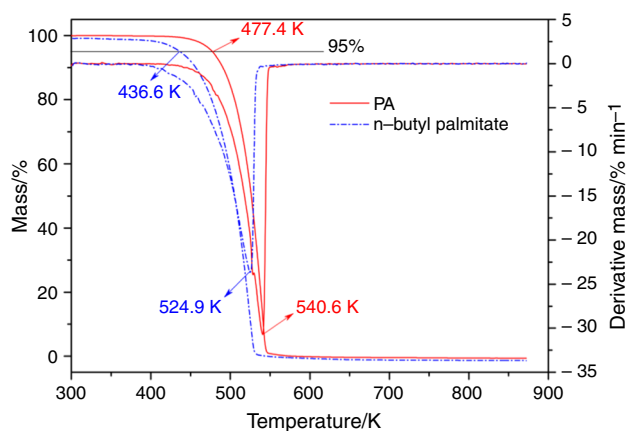
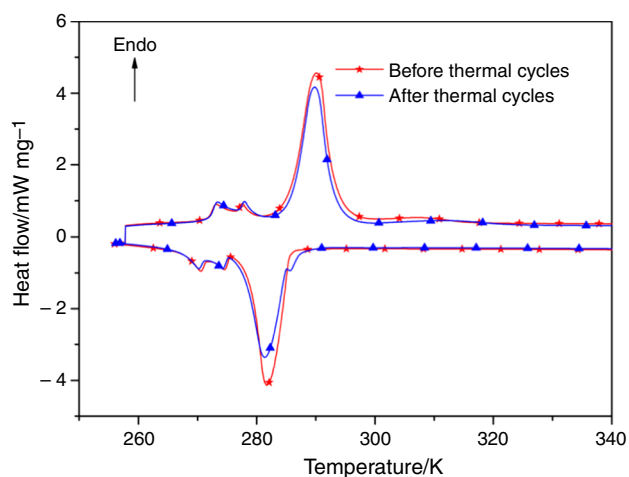


Fig. 5 TG and DTG curves of the PA and *n*-butyl palmitate

**Table 3** Thermal characteristics of the *n*-butyl palmitate before and after 500 thermal cycles

|                           | Melting process |                       | Cooling process |                       |
|---------------------------|-----------------|-----------------------|-----------------|-----------------------|
|                           | $T_m/K$         | $\Delta H_m/J g^{-1}$ | $T_c/K$         | $\Delta H_c/J g^{-1}$ |
| Before 500 thermal cycles | 285.6           | 127.1                 | 285.7           | 134.5                 |
| After 500 thermal cycles  | 286.5           | 113.5                 | 285.4           | 128.0                 |



**Fig. 6** DSC curves of the *n*-butyl palmitate before and after 500 thermal cycles

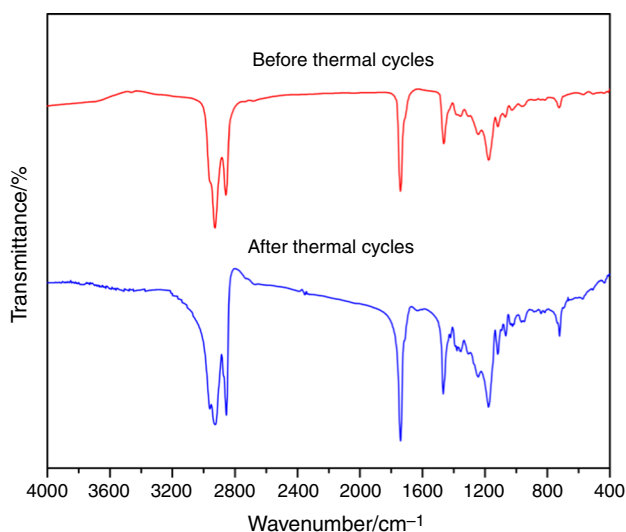


**Fig. 7** FTIR spectra of *n*-butyl palmitate before and after 500 thermal cycles

Table 3 further illustrated that the melting temperature of the *n*-butyl palmitate changed as + 0.9 K and the cooling temperature also changed to − 0.3 K. Furthermore, the latent heat of melting for *n*-butyl palmitate just changed by 10.7% and the latent heat of cooling just changed by 4.8% after 500 thermal cycles. The changes in the latent heats of melting and cooling of the *n*-butyl palmitate after thermal cycling were at a reasonable range for a PCM [16]. Therefore, the prepared *n*-butyl palmitate had superior thermal reliability.

In addition, from the FT-IR spectra in Fig. 7, there are no new chemical bond was observed after 500 thermal cycles. It was just a peak intensity shift, because the mass of the samples before thermal cycling was fewer than the after. The process of thermal cycle is the process of

segment rupture and recombination for the phase change material, there is no new chemical reaction observed. As a result, the synthesized *n*-butyl palmitate had relatively excellent thermal reliability during utility period.

## Conclusions

In this study, a type of PA ester was investigated as an organic PCM for LHTES. This PA ester called *n*-butyl palmitate was synthesized by the esterification reaction of PA with *n*-butanol. The prepared *n*-butyl palmitate and its components were systematically characterized by the FT-IR, <sup>1</sup>H NMR, DSC, Hot-disk, and TG techniques. The results revealed that the PA and *n*-butanol have reacted fully due to the new ester bond appeared. The DSC results suggested that the *n*-butyl palmitate had a suitable temperatures and high latent heats for melting or cooling. It is further explained that synthesized *n*-butyl palmitate can be utilized as a PCM for LHTES. Furthermore, the FT-IR and DSC analyses results displayed that there is no any degradation occurred in the chemical structure of the *n*-butyl palmitate after the duplicated 500 thermal cycles and no any significant change in thermal properties of the *n*-butyl palmitate, respectively. Therefore, as long as the thermal conductivity was enhanced by adding high thermal conductivity materials, the *n*-butyl palmitate can be used in many applications due to their suitable phase change temperature, satisfactory thermal properties, and good thermal reliability.

**Acknowledgements** This work was financially supported by the National Natural Science Foundation of China (31570572, 31670516 and 31600459).

## References

- Sarı A, Biçer A, Lafçı Ö, Ceylan M. Galactitol hexa stearate and galactitol hexa palmitate as novel solid-liquid phase change materials for thermal energy storage. *Sol Energy*. 2011;85:2061–71.
- Dheep GR, Sreekumar A. Investigation on thermal reliability and corrosion characteristics of glutaric acid as an organic phase change material for solar thermal energy storage applications. *Appl Therm Eng*. 2018;129:1189–96.
- Cui WW, Zhang HZ, Xia YP, Zou YJ, Xiang CL, Chu HL, Qiu SJ, Xu F, Sun LX. Preparation and thermophysical properties of a novel form-stable CaCl<sub>2</sub>·6H<sub>2</sub>O/sepiolite composite phase change material for latent heat storage. *J Therm Anal Calorim*. 2018;131(1):57–63.
- Jradi M, Gillott M, Riffat S. Simulation of the transient behaviour of encapsulated organic and inorganic phase change materials for low-temperature energy storage. *Appl Therm Eng*. 2013;59(1–2):211–22.
- Mahfuz MH, Anisur MR, Kibria MA, Saidur R, Metselaar IHSC. Performance investigation of thermal energy storage system with

- Phase Change Material (PCM) for solar water heating application. *Int Commun Heat Mass*. 2014;57:132–9.
- Genc M, Genc ZK. Microencapsulated myristic acid-fly ash with TiO<sub>2</sub> shell as a novel phase change material for building application. *J Therm Anal Calorim*. 2018;131:2373–80.
  - Zheng L, Zhang W, Liang F. A review about phase change material cold storage system applied to solar-powered air-conditioning system. *Adv Mech Eng*. 2017;9(6):1–20.
  - Deng Y, Li JH, Qian TT, Guan WM, Li YL, Yin XP. Thermal conductivity enhancement of polyethylene glycol/expanded vermiculite shape-stabilized composite phase change materials with silver nanowire for thermal energy storage. *Chem Eng J*. 2016;295:427–35.
  - Kaygusuz K, Sari A. Thermal energy storage performance of fatty acids as a phase change material. *Energ Sour A*. 2006;28(1–3):105–16.
  - Qu MJ, Guo CG, Li LP, Zhang XC. Preparation and investigation on tetradecanol and myristic acid/cellulose form-stable phase change material. *J Therm Anal Calorim*. 2017;130:781–90.
  - Ma LY, Guo CG, Ou RX, Sun LC, Wang QW, Li LP. Preparation and characterization of modified porous wood flour/lauric-myristic acid eutectic mixture as a form-stable phase change material. *Energ Fuel*. 2018;32(4):5453–61.
  - Feldman D, Banu D, Hawes D. Low chain esters of stearic acid as phase change materials for thermal energy storage in buildings. *Sol Energy Mater Sol Cells*. 1995;36:311–22.
  - Karaipekli A, Sari A. Preparation and characterization of fatty acid ester/building material composites for thermal energy storage in buildings. *Energ Build*. 2011;43(8):1952–9.
  - Sari A, Biçer A, Karaipekli A, Alkan C, Karadag A. Synthesis, thermal energy storage properties and thermal reliability of some fatty acid esters with glycerol as novel solid–liquid phase change materials. *Sol Energy Mater Sol Cells*. 2010;94(10):1711–5.
  - Sari A, Eroglu R, Biçer A, Karaipekli A. Synthesis and thermal energy storage properties of erythritol tetrastearate and erythritol tetrapalmitate. *Chem Eng Technol*. 2011;34(1):87–92.
  - Sari A, Karaipekli A. Preparation, thermal properties and thermal reliability of palmitic acid/expanded graphite composite as form-stable PCM for thermal energy storage. *Sol Energy Mater Sol Cells*. 2009;93(5):571–6.
  - Zhang H, Gao XN, Chen CX, Xu T, Fang YT, Zhang ZG. A capric-palmitic-stearic acid ternary eutectic mixture/expanded graphite composite phase change material for thermal energy storage. *Compos A Appl Sci Manuf*. 2016;87:138–45.
  - Sari A. Thermal energy storage properties of mannitol-fatty acid esters as novel organic solid-liquid phase change materials. *Energ Convers Manag*. 2012;64:68–78.
  - Li LP, Wang G, Guo CG. Influence of intumescent flame retardant on thermal and flame retardancy of eutectic mixed paraffin/polypropylene form-stable phase change materials. *Appl Energy*. 2016;162:428–34.
  - Guan WM, Li JH, Qian TT, Wang X, Deng Y. Preparation of paraffin/expanded vermiculite with enhanced thermal conductivity by implanting network carbon in vermiculite layers. *Chem Eng J*. 2015;277:56–63.
  - Liu HB, Pei DF, Chen S, Cao RR, Zhang XX. Fabrication and characterization of diethylene glycol hexadecyl ether-grafted graphene oxide as a form-stable phase change material. *Thermochim Acta*. 2018;661:166–73.
  - Zhang N, Yuan YP, Wang X, Cao XL, Yang XJ, Hu SC. Preparation and characterization of lauric-myristic-palmitic acid ternary eutectic mixtures/expanded graphite composite phase change material for thermal energy storage. *Chem Eng J*. 2013;231:214–9.
  - Tian BQ, Yang WB, Luo LJ, Wang J, Zhang K, Fan JH, Wu JY, Xing T. Synergistic enhancement of thermal conductivity for expanded graphite and carbon fiber in paraffin/EVA form-stable phase change materials. *Sol Energy*. 2016;127:48–55.
  - Khadiran T, Hussein MZ, Zainal Z, Rusli R. Shape-stabilised n-octadecane/activated carbon nanocomposite phase change material for thermal energy storage. *J Taiwan Inst Chem E*. 2015;55:189–97.
  - Sari A, Biçer A, Karaipekli A. Synthesis, characterization, thermal properties of a series of stearic acid esters as novel solid–liquid phase change materials. *Mater Lett*. 2009;63:1213–6.
  - Raghunanan L, Floros MC, Narine SS. Thermal stability of renewable diesters as phase change materials. *Thermochim Acta*. 2016;644:61–8.
  - Meng JY, Tang XF, Zhang ZL, Zhang XX, Shi HF. Fabrication and properties of poly(polyethylene glycol octadecyl ether methacrylate). *Thermochim Acta*. 2013;574:116–20.